Double-Plane Steps in Rectangular Waveguides and their Application for Transformers, Irises, and Filters

HARTMUT PATZELT AND FRITZ ARNDT

Abstract—**Double-plane steps in rectangular waveguides are investigated with the method of field expansion into eigenmodes. This method takes into account the influence of evanescent fields and power transmission due to higher order modes. The scattering coefficients of a *P*- (*Ku*-) to *X*-band waveguide transition as well as of resonant irises with finite thickness are calculated and compared with measured results. An optimum short double-plane three-section transformer is designed which shows equal-ripple behavior in passband. The performance of a reactance-coupled four resonator half-wave filter is improved by additional optimized double-plane steps.**

I. Introduction

DOUBLE-PLANE steps in rectangular waveguides play a significant role for the design of waveguide transformers [1]–[5], iris coupling structures [1], [2], [6], and waveguide filters [2]. For transformers, additional steps in the *H*-plane can yield shorter section lengths and lower reflection coefficients [2] in comparison with the mere *E*-plane type; rectangular irises of finite width and thickness can be used for tunable direct-coupled resonator filters [2]; the performance of reactance coupled half-wave waveguide filters can be improved by additional double-plane steps [2]. But there still exists a paucity of suitable theoretical research on such double-plane step circuits, including excitation of higher order modes which may influence considerably design data even below their cutoff frequency.

The investigations on waveguide transformers in [1] through [5] are based on the assumption that only the TE_{10} mode is propagating along the line. Therefore, no direct design of correct transformer section lengths is possible. For *E*-plane waveguide transformers there are empirical formulas for length correction; for double-plane transformers the designer is left to individual measurements [2]. Rectangular irises are usually calculated by equivalent circuit methods [2], [6]. Especially for thick irises, however, this first-order theory leads to wrong results if no empirical correction is included. Reactance-coupled half-wave (pseudo-high-pass) filters work well up to step discontinuity VSWR's in the neighborhood of 2 [2]. For other values there is a noticeable deviation from an equal-ripple response, which can be compensated by additional double-plane steps. The design values of [2], however, based on the quarter-wave transformer prototype, are not optimum, since higher order modes influence the effective resonator lengths and the step dimensions.

The theory given in this paper, which includes higher order mode excitation also below cutoff frequency, avoids these disadvantages and yields correct design data. It is based on field expansion into orthogonal eigenmodes [7], by which *E*-plane steps [8], [10], and infinitely thin inductive or capacitive irises [9] have already been investigated. In contrast to [8] through [10], however, double-plane step circuits require all field components to be considered.

Calculation of the scattering coefficients of dominant mode and next higher order modes for a transition of *P*- (*Ku*-) to *X*-band waveguide as well as for resonant irises with finite thickness demonstrates the influence of higher order mode propagation. The Fletcher–Powell optimization procedure [11] together with the higher order mode design theory leads directly to optimum double-plane stepped waveguide transformers and double-plane step compensated reactance-coupled half-wave filters. Measured results verify the theory.

II. Theory

For the double-plane step (Fig. 1(a)), the field is derived from the axial *z*-components of the magnetic and electric Hertzian vector potentials Π_h and Π_e [12]

$$\boldsymbol{E} = -j\omega\mu\nabla\times\boldsymbol{\Pi}_{hz} + \nabla\times\nabla\times\boldsymbol{\Pi}_{ez}$$

$$\boldsymbol{H} = j\omega\epsilon\nabla\times\boldsymbol{\Pi}_{ez} + \nabla\times\nabla\times\boldsymbol{\Pi}_{hz}. \tag{1}$$

The Hertzian potentials can be written as a sum of the products of the eigenfunctions $T^{(\nu)}_{h,e}(x, y)$ and the propagation expressions $\exp(\pm\gamma^{(\nu)}_{h,e}z)$ due to each mode excited at the step discontinuity between the two waveguides $\nu = 1$ and 2 (Fig. 1(a))

$$\Pi^{(\nu)}_{hz} = \sum_{m=0}^{\infty}\sum_{n=0}^{\infty} a^{(\nu)}_{hmn}T^{(\nu)}_{hmn} \cdot\exp\left(-\gamma^{(\nu)}_{hmn}z\right) + b^{(\nu)}_{hmn}T_{hmn}\exp\left(+\gamma^{(\nu)}_{hmn}z\right)$$

$$\Pi^{(\nu)}_{ez} = \sum_{m=1}^{\infty}\sum_{n=1}^{\infty} a^{(\nu)}_{emn}T^{(\nu)}_{emn} \cdot\exp\left(-\gamma^{(\nu)}_{emn}z\right) + b^{(\nu)}_{emn}T_{emn}\exp\left(+\gamma^{(\nu)}_{emn}z\right). \tag{2}$$

Manuscript received August 18, 1981; revised December 1, 1981.

H. Patzelt is with AEG-Telefunken GmbH., Department of Naval Technology, Hafenstrasse 32, D-2000 Wedel, West Germany.

F. Arndt is with the Microwave Department, University of Bremen, Kufsteiner Strasse NW 1, D-28000 Bremen, West Germany.

0018-9480/82/0500-0771$00.75 ©1982 IEEE

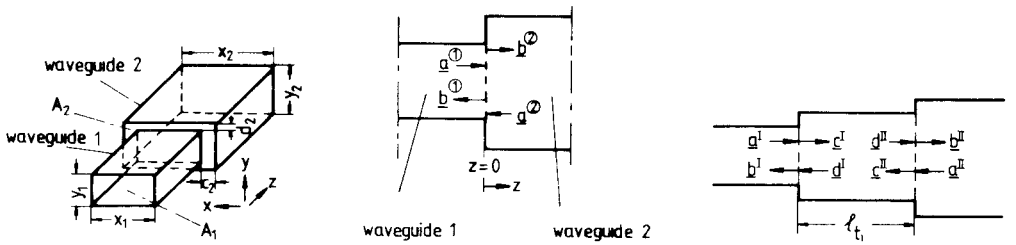

Fig. 1. Double-plane step in rectangular waveguide. (a) Step dimensions. (b) Forward and backward waves at the step. (c) Transformer section of two steps.

As in [13], the eigenfunctions are so normalized that the power carried by a given wave is proportional to the square of the wave-amplitude coefficients a and b

$$T_{hkl}^{(1)}=\frac{2\cdot\cos\left(k_x^{(1)}\cdot(x-c_2)\right)\cdot\cos\left(k_y^{(1)}\cdot(y-d_2)\right)}{N_1\cdot\sqrt{1+\delta_{0,k}}\cdot\sqrt{1+\delta_{0,l}}}$$

$$T_{ekl}^{(1)}=\frac{2\cdot\sin\left(k_x^{(1)}\cdot(x-c_2)\right)\cdot\sin\left(k_y^{(1)}\cdot(y-d_2)\right)}{N_1}$$

$$T_{hij}^{(2)}=\frac{2\cdot\cos\left(k_x^{(2)}\cdot x\right)\cdot\cos\left(k_y^{(2)}\cdot y\right)}{N_2\cdot\sqrt{1+\delta_{0,i}}\cdot\sqrt{1+\delta_{0,j}}}$$

$$T_{eij}^{(2)}=\frac{2\cdot\sin\left(k_x^{(2)}\cdot x\right)\cdot\sin\left(k_y^{(2)}\cdot y\right)}{N_2} \tag{3}$$

where $m=k$ and $n=l$ for $\nu=1$; $m=i$ and $n=j$ for $\nu=2$) with

$$N_1=\sqrt{x_1\cdot y_1}\cdot\sqrt{k_x^{(1)^2}+k_y^{(1)^2}}$$

$$N_2=\sqrt{x_2\cdot y_2}\cdot\sqrt{k_x^{(2)^2}+k_y^{(2)^2}}$$

$$k_x^{(1)}=\frac{k\cdot\pi}{x_1}\qquad k_y^{(1)}=\frac{l\cdot\pi}{y_1}$$

$$k_x^{(2)}=\frac{i\cdot\pi}{x_2}\qquad k_y^{(2)}=\frac{j\cdot\pi}{y_2} \tag{4}$$

where $x_1\leqslant x_2$, $y_1\leqslant y_2$ and

$$\gamma_{h,emn}^{(\nu)}=jk\sqrt{1-\frac{\left(k_{xmn}^{(\nu)}\right)^2+\left(k_{ymn}^{(\nu)}\right)^2}{k^2}}$$

$k=\omega\sqrt{\mu\epsilon}$, and $\delta_{0,n}=$ Kronecker delta.

The still unknown coefficients a and b in (2) correspond directly to normalized incident and reflected waves related to each other by the scattering matrix which can be determined by matching the fields at the step discontinuity at $z=0$ (Figs. 1(a) and 1(b))

$$E_{x,y}^{(1)}\Big|_{\substack{z=0\\A_1}}=E_{x,y}^{(2)}\Big|_{\substack{z=0\\A_1}}\qquad E_{x,y}^{(2)}\Big|_{\substack{z=0\\A_2-A_1}}=0$$

$$H_{x,y}^{(1)}\Big|_{\substack{z=0\\A_1}}=H_{x,y}^{(2)}\Big|_{\substack{z=0\\A_1}}. \tag{5}$$

This leads to the matrix equation (see Appendix, where also the abbreviations $V_{h,h}$, $V_{h,e}$, $V_{h,e}$, and $V_{e,e}$ are explained; $U=$ unit matrix)

$$\underbrace{\begin{bmatrix} U & \begin{matrix} V_{h,h}^T & V_{h,e}^T \\ 0\ \cdots\ 0 & \\ \vdots\ \ddots\ \vdots & V_{e,e}^T \\ 0\ \cdots\ 0 & \end{matrix} \\ \begin{matrix} 0\ \cdots\ 0 \\ V_{h,h}\ \vdots\ \ddots\ \vdots \\ 0\ \cdots\ 0 \end{matrix} & -U \\ V_{e,h} \quad V_{e,e} & \end{bmatrix}}_{K_1}\cdot\underbrace{\begin{bmatrix} a_h^{(1)} \\ \vdots \\ a_e^{(1)} \\ \vdots \\ a_h^{(2)} \\ \vdots \\ a_e^{(2)} \\ \vdots \end{bmatrix}}_{a}=\underbrace{\begin{bmatrix} U & \begin{matrix} V_{h,h}^T & V_{h,e}^T \\ 0\ \cdots\ 0 & \\ \vdots\ \ddots\ \vdots & V_{e,e}^T \\ 0\ \cdots\ 0 & \end{matrix} \\ \begin{matrix} 0\ \cdots\ 0 \\ -V_{h,h}\ \vdots\ \ddots\ \vdots \\ 0\ \cdots\ 0 \end{matrix} & U \\ -V_{e,h} \quad -V_{e,e} & \end{bmatrix}}_{K_2}\cdot\underbrace{\begin{bmatrix} b_h^{(1)} \\ \vdots \\ b_e^{(1)} \\ \vdots \\ b_h^{(2)} \\ \vdots \\ b_e^{(2)} \\ \vdots \end{bmatrix}}_{b} \tag{6}$$

The scattering matrix of the step discontinuity (Fig. 1(b)) is then given by

$$S=\left[\begin{array}{c|c} S_{11} & S_{12} \\ \hline S_{21} & S_{22} \end{array}\right]=K_2^{-1}\cdot K_1. \tag{7}$$

A series of steps (see Fig. 1(c)) is commonly treated by transmission matrix parameters, e.g., [3]. But this is not appropriate, if, like here, higher order modes are included

which are excited below their cutoff frequency. Since transmission matrix parameters for certain frequencies then may contain exponential functions with positive argument they exceed for many geometrical cases the available numerical range of the computer. The direct combination of the involved scattering matrices is numerically stable as is shown for two steps (Fig. 1(c)) as an example, only containing exponential functions with negative arguments

$$\begin{bmatrix} b^{\mathrm{I}} \\ b^{\mathrm{II}} \end{bmatrix} = \left(\begin{bmatrix} S_{11}^{\mathrm{I}} & 0 \\ 0 & S_{22}^{\mathrm{II}} \end{bmatrix} + \begin{bmatrix} S_{12}^{\mathrm{I}} D & 0 \\ 0 & S_{21}^{\mathrm{II}} \end{bmatrix} \begin{bmatrix} E S_{11}^{\mathrm{II}} D & E \\ F & F S_{22}^{\mathrm{I}} D \end{bmatrix} \cdot \begin{bmatrix} S_{21}^{\mathrm{I}} & 0 \\ 0 & S_{12}^{\mathrm{II}} \end{bmatrix} \right) \begin{bmatrix} a^{\mathrm{I}} \\ a^{\mathrm{II}} \end{bmatrix} \quad (8)$$

where I and II denote the steps I and II, respectively, and

$$E = \left(U - S_{11}^{\mathrm{II}} D S_{22}^{\mathrm{I}} D\right)^{-1}$$

$$F = \left(U - S_{22}^{\mathrm{I}} D S_{11}^{\mathrm{II}} D\right)^{-1}$$

where U = unit matrix, and D = diagonal matrix with

$$D_{ii} = e^{-\gamma_i \cdot l_{ii}}$$

due to the transformer sections of length l_{ii} between the double steps, (see Fig. 1(c)). Besides the numerical stability, a further advantage of this direct calculation in comparison with the transmission parameter method is that no symmetry of ports (i.e., waves) is required. A series of more than two steps can be treated analogous to (8).

For double-plane steps with excentric waveguide axes, the $H_{10}(\mathrm{TE}_{10})$ wave incident excites all $H_{mn}(\mathrm{TE}_{mn})$ and $E_{mn}(\mathrm{TM}_{mn})$ waves with $m = (0), 1, 2, 3, \cdots$, and $n = (0), 1, 2, 3, \cdots, (m = 0$ or or $n = 0$ only for $\mathrm{TE}_{mn})$. If the axes are concentric, only the waves $m = 1, 3, 5, \cdots$, and $n = (0), 2, 4, 6, \cdots$, are excited. Because of limited computing time and storage requirements, the number of series terms in (2), i.e., the number of modes considered, has to be restricted to finite values M and N, respectively. The maximum values necessary for computing the examples described are $M = 9$ and $N = 8$, respectively, for double-plane steps.

III. Results

The first example investigated is the step discontinuity of a *P*- (*Ku*-)band waveguide (12.4–18 GHz, $x_1 = 15.8$ mm, $y_1 = 7.9$ mm, see Fig. 1(a)) to an *X*-band waveguide (8.2–12.4 GHz, $x_2 = 22.9$ mm, $y_2 = 10.2$ mm). The magnitude of the calculated scattering coefficients for the first wavetypes is shown in Fig. 2. S_{11} together with the wavetype in round brackets denotes the corresponding reflection coefficient, S_{21} the corresponding transmission coefficient, if an H_{10} wave is incident in the *P*-band waveguide. It can be stated that a high amount of energy is transported by higher order modes.

In this example, the inclusion of higher order modes up to $M = 5$ and $N = 4$ has turned out to yield sufficient convergence behavior (within drawing-accuracy) of the scattering coefficients. For comparison, $|S_{11}|_{(H_{10})}$ has been measured in the frequency range of 10–18 GHz showing good agreement with theoretical results.

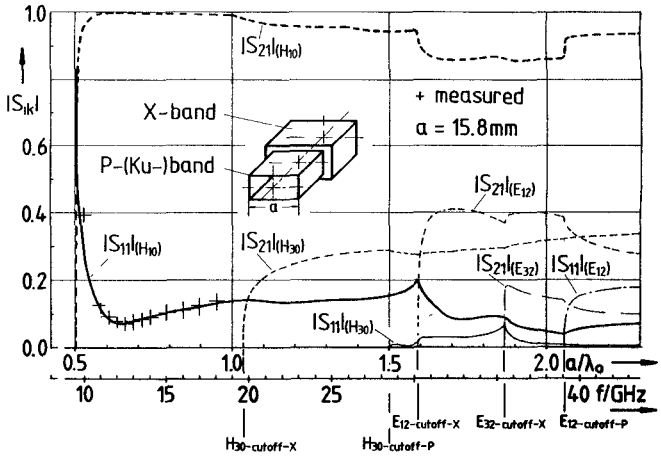

Fig. 2. Scattering coefficients as a function of normalized free-space wavelength and frequency, respectively, of a concentric step discontinuity from a *P*- (*Ku*-) band to an *X*-band waveguide if a H_{10} (TE_{10}) wave is incident. $|S_{11}|_{(H_{10})}$ = magnitude of reflection coefficient, H_{10}-wave, $|S_{21}|_{H_{30}}$ = magnitude of transmission coefficient, H_{30}-wave, etc., $H_{10\text{-cutoff-}P}$ = cutoff frequency of the H_{10}-wave in the *P*-band waveguide, etc., λ_0 = free-space wavelength, $a = x_1 = 15.8$ mm, $y_1 = 7.9$ mm; $x_2 = 22.9$ mm, $y_2 = 10.2$ mm, see Fig. 1(a).

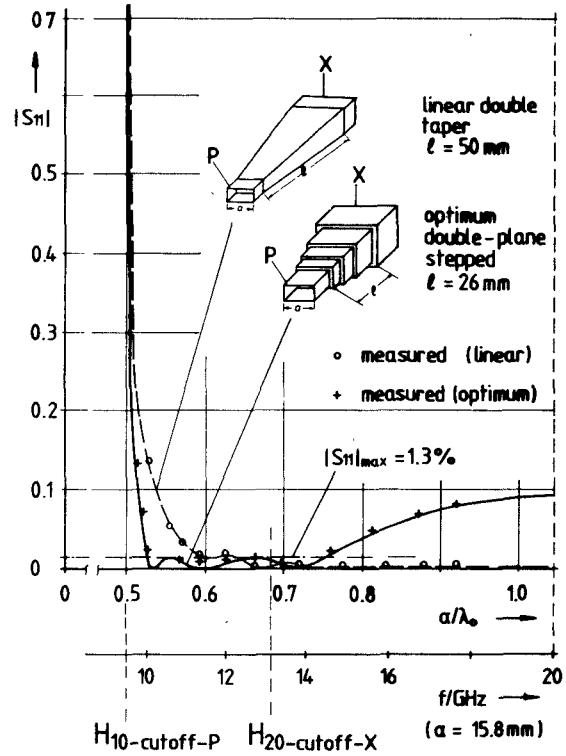

Fig. 3. Magnitude of the reflection coefficient of double-plane transformers between a *P*- and an *X*-band waveguide. – – – linear double taper approximated by 24 steps. —— optimum double-plane stepped (design data see Table I).

Double-plane (inhomogeneous) transformers come about, for instance, when rectangular waveguides having different heights and widths are cascaded. Also, inhomogeneous transformers may serve as taper section when rectangular waveguides are combined with ridged, circular, or other types of waveguide.

In [5], linearly double tapered waveguide transformers are suggested. Fig. 3 shows the calculated and measured

reflection coefficient of such a transformer (dashed line). As an example of application, such as in Fig. 2, a waveguide transition from P-band to X-band is chosen, and the length of the transformer section is assumed to be $l = 50$ mm. For calculation, the taper is subdivided into 24 steps of equal lengths, where each step yields a scattering matrix according to (7); the series is calculated following (8).

As can be stated, the liner taper is not optimum concerning the length of the coupling section and reflection behavior. Moreover, the high-pass behavior of this continuously tapered structure cannot be taken advantage of since the range of suitable waveguide application is limited by the cutoff frequency of the $H_{20}(TE_{20})$ wave in the broader (X-band) waveguide. Therefore, an optimum short three-section double-plane transformer is proposed which shows nearly Tchebycheff behavior of the reflection coefficient in passband (Fig. 3, solid line). The design data are calculated with the Fletcher–Powell method [11] by minimizing the error function

$$F(\bar{x}) = \sum_{j=1}^{J} \frac{|S_{11}(\bar{x}, f_j)|^2}{|S_{21}(\bar{x}, f_j)|^2} \tag{9}$$

with the parameter vector

$$\bar{x} = (x_1, x_2, x_3, \cdots, x_n; y_1, y_2, y_3, \cdots, y_n; l_{t1}, l_{t2}, l_{t3}, \cdots, l_{tn})^T$$

f_j = frequency sample points, x_i = height, y_i = width, l_{ti} = length of the transformer section i, and with the scattering parameters according to (7) and (8). The optimum design data are given in Table I.

In Fig. 3, for each step discontinuity, as in Fig. 2, the number of waves M and N, in (2), is chosen to be $M = 5$ and $N = 4$. The waves, however, within the waveguide sections of length l_{ti} (see Fig. 1(c) and diagonal matrix D in (8)) are taken into account according to increasing cutoff frequency. Seven consecutive waves (TE_{10}, TE_{30}, TE_{12}, TM_{12}, TE_{32}, TM_{32}, and TE_{50}) have turned out to be sufficient to yield adequate convergence behavior for the examples in Fig. 3, since the fringing fields due to modes of still higher order, evanesce relatively quickly with distance because of the described technique of directly combining the scattering matrices according to (8).

Fig. 4 shows the scattering parameters of resonant irises with finite thickness. Also, here the considerable amount of energy transported by higher order modes is demonstrated. By measurement, it is shown that the calculated values (e.g., the resonant frequency) are in close coincidence with practice. For these examples, M and N are assumed to be $M = 7$ and $N = 8$. Seven consecutive waves have been taken into account within the iris waveguide section.

In [2], reactance-coupled pseudo-high-pass filters are improved by two additional double-plane steps. Fig. 5 (dashed line) shows the transmission coefficient in decibels calculated with (7) and (8) for dimensions according to [2] (see Table I). It can be stated that in contrast to the theoretical predicted performance in [2] no optimum response is obtained. An optimization however, according to (9) leads to

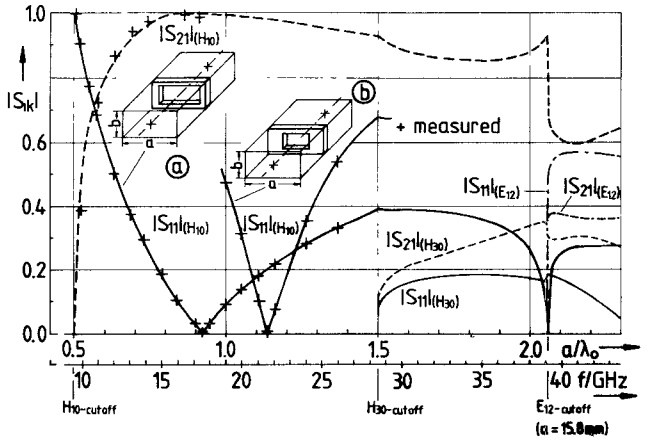

Fig. 4. Magnitude of the scattering coefficients of resonant irises with finite thickness t. Waveguide dimensions: $a = 15.8$ mm, $b = 7.9$ mm (P-(Ku-) band). Iris dimensions: ⓐ: $a' = a\sqrt{2}$, $b' = b/\sqrt{2}$, $t = 2$ mm; ⓑ: $a' = a/2$, $b' = b/2$, $t = 2$ mm. (For iris ⓑ only $S_{11(H_{10})}$ in the near of resonant frequency is shown.)

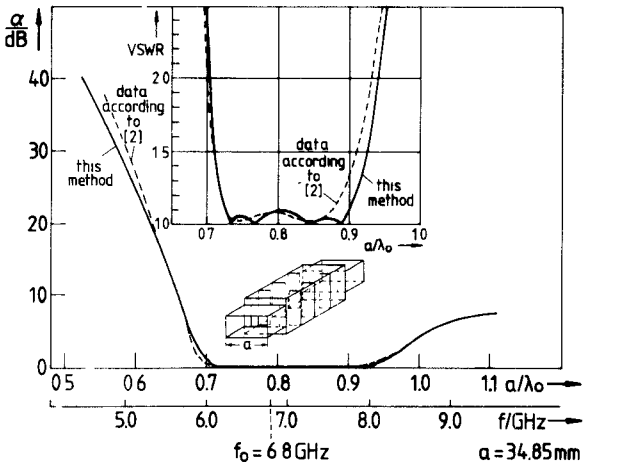

Fig. 5. Transmission coefficient $\alpha = -20\log|S_{21}|$ in decibels of a reactance-coupled four resonator half-wave pseudo-high-pass filter with double-step compensation. – – – design data according to [2] (see Table I). —— optimized design data (see Table I).

TABLE I
DIMENSIONS OF DESIGNED TRANSFORMERS AND FILTERS

Optimum double-plane three-section transformer (Fig. 3)					
	waveguide 1	section 1	section 2	section 3	waveguide 2
a/mm[1]	15.8	17.57	19.33	21.09	22.86
b/mm	7.9	8.47	9.03	9.60	10.16
l_t/mm		9.72	8.83	8.29	
	(P-(Ku-)band)				(X-band)

Reactance coupled half-wave filter (Fig. 5)							
		waveguide 1 and 2	iris 1,5	res.1,4	iris 2,4	res.2,3	iris 3
not optimized according to [2]	a/mm[1]	34.85	24.484	34.85	19.142	34.85	17.493
	b/mm	15.8	23.7	23.7	23.7	23.7	23.7
	l_r/mm		0	17.057	0	19.265	0
optimized	a/mm	34.85	29.190	34.85	19.142	34.85	17.493
	b/mm	15.8	24.5	24.5	24.5	24.5	24.05
	l_r/mm		0	23.444	0	19.265	

1) a = width, b = height, l_t = lenght of transformer section, l_r = length of resonator

optimum design data (see Table I) which provide nearly equal-ripple behavior (Fig. 5, solid line). For these examples, M and N are chosen to be $M = 9$ and $N = 8$ for each

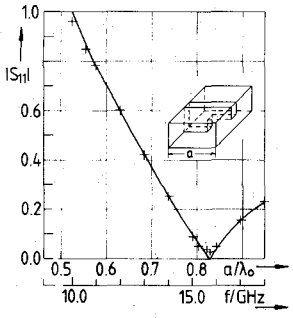

Fig. 6. Magnitude of the reflection coefficient of an unsymmetrical resonant iris if an H_{10} wave is incident. Waveguide dimensions: $x_1 = 15.8$ mm, $y_1 = 7.9$ mm. Iris dimensions: $x_2 = 11.85$ mm, $y_1 = 6$ mm, thickness $= 3$ mm.

step. But since the resonator lengths between them are relatively long, only three consecutive waves have turned out to be sufficient within these sections for the frequency range considered.

To demonstrate the application of the method described for a double step with excentric axes, an unsymmetrical resonant iris with finite thickness is chosen. Fig. 6 shows the calculated and measured magnitude of the scattering coefficient S_{11} for an incident TE_{10} wave. M and N are each chosen to be equal to 4 (note that all modes are excited). Five consecutive waves are considered within the iris waveguide section.

Further examples for a treatment with this method are inductive and capacitive irises with finite thickness. If only a TE_{10} wave is incident (note that this is not the case for the pseudo-high-pass filter irises in Fig. 5), for an inductive iris only TE_{m0}, for a capacitive iris only TE_{1n} and TM_{1n} waves are excited. Sufficient convergence behavior and coincidence with measurements is obtained for $M = 25$ (inductive iris) and $N = 12$ (capacitive iris) as well as five consecutive waves within the iris (iris dimensions up to one-half of the corresponding waveguide dimensions provided, and thickness not less than about one-tenth of the iris dimension).

IV. Conclusions

A design theory for double-plane steps in rectangular waveguides is suggested which takes into account higher order mode excitation also below cutoff frequency. This allows one to include in the design procedure the influences of fringing fields as well as of transmission coefficients due to higher order mode propagation. At the example of a double-plane step from P- (Ku-) band to X-band waveguide as well as of resonant irises the high amount of higher order mode propagation can be demonstrated.

An optimum double-plane three-step transformer for a P- to X-band waveguide is designed which shows equal-ripple behavior in passband and requires about half the transformer length as, e.g., a linear double taper calculated for comparison.

Reactance-coupled pseudo-high-pass filters can be improved by additional double-plane steps. But the hitherto known design data are not optimum. If higher order mode excitation is considered in the design process, as is demonstrated, a nearly equal-ripple behavior is obtained.

The eigenmode expansion method described converges relatively quickly. But to avoid adding unnecessary computing time and storage requirements, in the general eigenmode expression, the preselection of excited modes, due to symmetry conditions and to the wave incident, is advantageous. For the practically important "coaxial" double steps, as well as for inductive and capacitive irises, the excited modes are denominated.

Instead of treatment with transmission matrix parameters, a series of steps is treated by a direct combination of the involved scattering matrices only containing exponential functions with negative arguments. Beyond numerical stability, this yields the further advantage that fringing fields of higher order modes below their cutoff frequency evanesce relatively quickly with distance. This reduces the number of modes to be considered between step discontinuities for distances being long compared with guide wavelength.

Acknowledgment

The authors wish to express their thanks to Dr. Grauerholz for technical assistance and precise measurements.

Appendix

Equations (1)–(5) lead to the following equations:

$$\mathbf{a}^{(1)}_{hij} + \sum_{k=0}^{\infty}\sum_{l=0}^{\infty} \mathbf{V}^{T}_{hhijkl}\mathbf{a}^{(2)}_{hkl} + \sum_{k=1}^{\infty}\sum_{l=1}^{\infty} \mathbf{V}^{T}_{heijkl}\mathbf{a}^{(2)}_{ekl} = \mathbf{b}^{(1)}_{hij} + \sum_{k=0}^{\infty}\sum_{l=0}^{\infty} \mathbf{V}^{T}_{hhijkl}\mathbf{b}^{(2)}_{hkl} + \sum_{k=1}^{\infty}\sum_{l=1}^{\infty} \mathbf{V}^{T}_{heijkl}\mathbf{b}^{(2)}_{ekl} \tag{A1}$$

$$\mathbf{a}^{(1)}_{eij} + \sum_{k=1}^{\infty}\sum_{l=1}^{\infty} \mathbf{V}^{T}_{eeijkl}\mathbf{a}^{(2)}_{ekl} = \mathbf{b}^{(1)}_{eij} + \sum_{k=1}^{\infty}\sum_{l=1}^{\infty} \mathbf{V}^{T}_{eeijkl}\mathbf{b}^{(2)}_{ekl} \tag{A2}$$

$$\sum_{k=0}^{\infty}\sum_{l=0}^{\infty} \mathbf{V}_{hhijkl}\mathbf{a}^{(1)}_{hkl} - \mathbf{a}^{(2)}_{hij} = \sum_{k=0}^{\infty}\sum_{l=0}^{\infty} -\mathbf{V}_{hhijkl}\mathbf{b}^{(1)}_{hkl} + \mathbf{b}^{(2)}_{hij} \tag{A3}$$

$$\sum_{k=0}^{\infty}\sum_{l=0}^{\infty} \mathbf{V}_{ehijkl}\mathbf{a}^{(1)}_{hkl} + \sum_{k=1}^{\infty}\sum_{l=1}^{\infty} \mathbf{V}_{eeijkl}\mathbf{a}^{(1)}_{ekl} - \mathbf{a}^{(2)}_{eij} = \sum_{k=0}^{\infty}\sum_{l=0}^{\infty} -\mathbf{V}_{ehijkl}\mathbf{b}^{(1)}_{hkl} + \sum_{k=1}^{\infty}\sum_{l=1}^{\infty} -\mathbf{V}_{eeijkl}\mathbf{b}^{(1)}_{ekl} + \mathbf{b}^{(2)}_{eij} \tag{A4}$$

with the abbreviations

$$\mathbf{V}_{hhijkl} = \sqrt{\frac{\gamma^{(2)}_{hij}}{\gamma^{(1)}_{hkl}}} \int_{A_1} \left(-\boldsymbol{e}^{(1)}_{hkl}\right)\left(-\boldsymbol{e}^{(2)}_{hij}\right) dx\, dy \tag{A5}$$

and

$$-\mathbf{V}_{heijkl}=\sqrt{\frac{\gamma_{hij}^{(2)}\gamma_{ekl}^{(1)}}{j\frac{2\pi}{\lambda}}}\int_{A_1}\left(\boldsymbol{e}_{ekl}^{(1)}\right)\left(-\boldsymbol{e}_{hij}^{(2)}\right)dx\,dy \quad \text{(A6)}$$

$$-\mathbf{V}_{ehijkl}=\sqrt{\frac{j\frac{2\pi}{\lambda}}{\gamma_{hkl}^{(1)}\gamma_{eij}^{(2)}}}\int_{A_1}\left(-\boldsymbol{e}_{hkl}^{(1)}\right)\left(\boldsymbol{e}_{eij}^{(2)}\right)dx\,dy \quad \text{(A7)}$$

$$\mathbf{V}_{eeijkl}=\sqrt{\frac{\gamma_{ekl}^{(1)}}{\gamma_{eij}^{(2)}}}\int_{A_1}\left(\boldsymbol{e}_{ekl}^{(1)}\right)\left(\boldsymbol{e}_{eij}^{(2)}\right)dx\,dy \quad \text{(A8)}$$

where A_1 = area of waveguide 1 (see Fig. 1(a)).

The vectors $\boldsymbol{e}$ denote

$$\boldsymbol{e}_{hkl}^{(1)}=\boldsymbol{e}_z\times\nabla_{xy}\mathbf{T}_{hkl}^{(1)} \quad \text{(A9)}$$

$$\boldsymbol{e}_{ekl}^{(1)}=\nabla_{xy}\mathbf{T}_{ekl}^{(1)} \quad \text{(A10)}$$

$$\boldsymbol{e}_{hij}^{(2)}=\boldsymbol{e}_z\times\nabla_{xy}\mathbf{T}_{hij}^{(2)} \quad \text{(A11)}$$

$$\boldsymbol{e}_{eij}^{(2)}=\nabla_{xy}\mathbf{T}_{eij}^{(2)}. \quad \text{(A12)}$$

$\mathbf{V}^T$ is the transposed matrix of $\mathbf{V}$.

References

[1] N. Marcuvitz, *Waveguide Handbook*. New York: McGraw-Hill, 1951.

[2] G. Matthaei, L. Young, and E. M. T. Jones, *Microwave Filters, Impedance-Matching Networks, and Coupling Structures*. New York: McGraw-Hill, 1964.

[3] S. B. Cohn, "Optimum design of stepped transmission-line transformers," *IRE Trans. Microwave Theory Tech.*, vol. MTT-3, pp. 16–21, Apr. 1955.

[4] H. J. Riblet, "General synthesis of quarter-wave impedance transformers," *IRE Trans. Microwave Theory Tech.*, vol. MTT-5, pp. 36–43, 1957.

[5] A. Chakraborty and G. S. Sanyal, "Transmission matrix of a linear double taper in rectangular waveguide," *IEEE Trans. Microwave Theory. Tech.*, vol. MTT-28, pp. 577–579, June 1980.

[6] M. S. Navarro, T. E. Rozzi, and Y. T. Lo, "Propagation in a rectangular waveguide periodically loaded with resonant irises," *IEEE Trans. Microwave Theory Tech.*, vol. MTT-28, pp. 857–865, Aug. 1980.

[7] H. Patzelt, "Berechnung von Querschnittssprüngen im Rechteckhohlleiter, inhomogenen Rechteckhohlleitertransformatoren, Blenden endlicher Dicke im Rechteckhohlleiter und längsgekoppelten rechteckhohlleiterfiltern mit der methode der Orthogonalreihenentwicklung," Dr.-Ing. dissertation, University of Bremen, Bremen, Germany, Oct. 1978.

[8] G. Piefke and R. Strube, "Reflexion und transmission beim Einfall einer H_{10}-welle auf eine sprunghafte Änderung eines Rechteckhohlleiters in der *E*-Ebene," *Arch. Elek. Übertragung*, vol. 19, pp. 231–243, 1965.

[9] H. D. Knetsch, "Anwendung der Methode der Orthogonalentwicklung bei unendlich dünnen Blenden in Hohlleitern," *Arch. Elek. Übertragung*, vol. 23, pp. 361–368, 1969.

[10] R. Safavi-Naini and R.H. MacPhie, "On solving waveguide junction scattering problems by the conservation of complex power technique," *IEEE Trans. Microwave Theory Tech.*, vol. MTT-29, pp. 337–343, Apr. 1981.

[11] R. Fletcher and M. J. D. Powell, "A rapidly convergent descent method for minimization," *Comput J.*, vol. 6, pp. 163–168, 1963.

[12] R. E. Collin, *Field Theory of Guided Waves*. New York: McGraw-Hill, 1960, ch. 1.6, pp. 22–27.

[13] F. Arndt and G.U. Paul, "The reflection definition of the characteristic impedance of microstrips," *IEEE Trans. Microwave Theory Tech.*, vol. MTT-27, pp 724–731, Aug. 1979.

Hartmut Patzelt was born in Breslau, Germany (now Wroclaw, Poland) in 1942. In 1970 he received the Engineer's degree in telecommunications from the Engineer School of Dortmund, West Germany. He received the Diplom. degree (telecommunications) and the Doctor Eng. degree from the University of Bremen, West Germany, in 1975 and 1978, respectively.

Since 1978 he has been with AEG-Telefunken GmbH., West Germany.

Fritz Arndt was born in Konstanz, Germany, on April 30, 1938. He received the Dipl.-Ing., the Dr.-Ing., and the Habilitation degrees from the Technical University of Darmstadt, Germany, in 1963, 1968, and 1972, respectively.

From 1963 to 1972 he worked on directional couplers and microstrip techniques at the Technical University of Darmstadt. Since 1972 he has been a Professor and Head of the Microwave Department at the University of Bremen, Germany. His research activities are at present in the area of the solution of field problems of waveguide and fin-line structures, of antenna design, and of microwave holography.

Dr. Arndt is member of the VDE and NTG (Germany). In 1970 he received the NTG award.